The Role of the Thumb: Study of Finger Motion in Grasping and Reachability Space in Human and Robotic Hands

Giuseppe Cotugno, Kaspar Althoefer, *Member, IEEE*, Thrishantha Nanayakkara, *Member, IEEE*

***Abstract*—It is well acknowledged that the opposing thumb granted humans advanced manipulation capabilities. However, such feature is not statistically quantified and its representation is not formally addressed in robotics yet. This paper studies whether the displacement of the opposing thumb in humans is a determining factor for shaping the grip. Using statistical analysis of the variability of motion capture data from the GRASP database, we found that the displacement of the thumb plays a leading role on the shaping of the grip, independently from the specific object being grasped. Furthermore, we map and compare the reachability spaces of the human thumb and two state-of-the-art robotic thumbs - the Shadow and the iCub hands. We conclude that the kinematics of robotic thumbs does not evenly span the reachability space of the human thumb, favouring precision grasping motions. Hence our findings contributes to the discussion of the optimal modelling of robotic hands.**

***Index Terms*—Kinematics, Multifingered Hands, Grasping, Dexterous Manipulation, Humanoid Robots.**

I. Introduction

SINCE mid-eighties, researchers tried to model the human hand functional features, such as grasping and object manipulation, for robotic multifingered grippers. For instance, the Okada hand [1] was one of the first examples of multifingered grippers developed for robotic applications. The human hand has attracted attention in robotics, as it is one of the most dexterous multifingered grippers available in nature, granting humans the ability to manipulate objects precisely. Additionally, every-day objects and tools are tailored for the functional needs of the human hand. Hence, a faithful robotic implementation of human grasping principles would allow robotic manipulation of such wide range of objects designed for human use without further modifications.

It is well known in the community of evolutionary biology [2], [3], that the most important advancement that granted manipulation skills to prehistoric humans and primates is the possibility to oppose the thumb towards the other fingers. The ability of opposing the thumb is an infrequent skill in nature, mostly developed in humans and some primates in different ways [4], [5]. The above mentioned studies highlight the importance of the opposition feature of the thumb but do not quantify the characteristics of its motion.

Manuscript received July XX, 2015; revised November xx, 2015.

Corresponding author: G. Cotugno (email: giuseppe.cotugno@kcl.ac.uk).

Authors are with the Centre for Robotics Research, School of Natural and Mathematical Sciences, King's College London, Strand WC2R 2LS, London, UK

Anatomical studies of the hand and the thumb have been conducted to understand the joint structure and the mechanisms of actuation of the fingers [6]. For instance, the opposition mechanism of the thumb is assessed through anatomical analysis of hand skeletal bones [7], or analysis of the variability of the trapeziometacarpal motion [8]. It is well acknowledged that the loss of the thumb corresponds to the loss of 40% of the hand function [9], however, a common agreement on the mechanics of the human thumb opposition has not been reached yet [10].

In robotics, several attempts to model the kinematics of the human hand and the thumb have been done in the past, settling the number of joints in between 15 [11] to 25 [12]. However, there is no general agreement on the best solution to create a model that renders the dynamics of human grasping and manipulation. Consequently, very different approaches are used to design robotic hands. Some solutions offer very advanced human-like kinematics, such as the Shadow hand [13]. Other human-like grippers, such as the DLR/HIT Hand [14], and human-inspired grippers, such as the Barret Hand [15], offer less degrees of freedom (DoFs), reduced number of fingers and, sometimes, a non-anthropomorphic kinematic design. Nevertheless the robotic hands with simpler or non-anthropomorphic kinematics are equally well established. A more recent trend is the implementation of grippers with under-actuated kinematics [16], [17]. The available robotics hands have differences on some fundamental kinematic design choices, such as the number of used and controlled fingers, the foldability of the palm and the reachability space of each finger. This suggests that some of the principal features of human grasping and manipulation skills are not fully explored and quantified yet.

The grasping capabilities of robotic grippers and human hands are evaluated and compared in order to understand better the main principles of grasping. For instance, [18] evaluates the kinematic space of the fingers as a whole, and [19] is addressing solutions to the correspondence problem for the entire hand. Such contributions are very important, but they don't take into account the prominent role of the thumb. Our previous studies [20], [21] indicate the importance of the thumb placement during grasping using a human-like robotic gripper (iCub hand). These findings were verified from grasping a set of everyday objects with different geometries.

Based on the existing literature and our previous studies, in the first part of the paper we are answering the question of whether the motion of the thumb influences the shaping of the

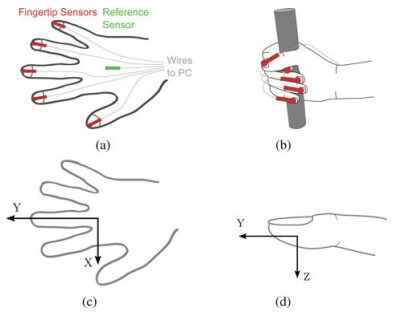

Fig. 1: Description of the set up of the sensors [18]. (a) Position of the sensors on the fingers (red) and of the reference sensor on the dorsum (green). (b) Example of grasp posture. (c) and (d) Coordinate system used in the analysis.

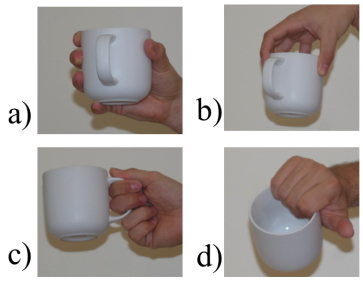

Fig. 2: Four posture classes based on the position of the thumb, a) Power Grasp, b) Precision Grasp, c) Key Grasp, d) Primate Grasp

grip independently from the specific object being grasped. The second part of this work studies how the reachability space of state-of-the-art robotic thumb kinematics maps to the human one using two well known robotic samples.

This paper is organized as follows: Section II presents the methodology of the analysis and a classification of grasping postures used in the paper. In Section III, our question on the role of the thumb in grasping is investigated by analysing the fingertip motions. Then, in Section IV the reachability space of the human thumb is compared with the reachability spaces of two robotic thumbs, and the representation of each grasp category is evaluated. Finally, Section V concludes our paper and highlights directions for future research.

II. Methodology

A. Methodology of the Analysis

To explore the role of the thumb in grasping, it is required to analyse the position of all fingertips for different postures across subjects. The dataset used for our analysis is described in the following subsection. The positions of the fingertips are expressed in the coordinate system of the reference frame. The centre of the reference frame is placed on the dorsum of each subject's hand, so that any motions of the wrist and the arm are eliminated. Figure 1 shows the orientation of the axes of the reference frame. The position of the fingertips is analysed and compared in three-dimensional space. Therefore, the rotation and translation components of each data point are combined together relative to the reference frame. For the analysis it was decided to use the displacements of the fingertips only, without using any additional information that a kinematic model of the hand could give. Using a kinematic model would impose an arbitrary structure that would bias the data making the analysis less general, since there is no agreement on the ideal kinematic model of the hand as mentioned in Section I.

Our statistical analysis is based on the evaluation of the standard deviation, covariance and mode of the covariance of the displacements of all digits across subjects. The full demonstration sequence - from the approaching to the retreating - is taken into account to analyse the complete motion of the fingertips during a grasping action. The analysis of variance (ANOVA) is used to evaluate whether there are factors that can significantly influence the displacement of the fingers, namely, the grasped object, the chosen posture, and the individual behaviour of each subject. The statistical evaluation was performed across 300 trials. Before this analysis, a Kolmogorov-Smirnov test was performed on every trial to test whether the data follows a Gaussian distribution. The results have shown that the data is normally distributed in all trials. In the ANOVA tests, the impact of the factor was considered significant in case the null hypothesis was rejected with 95% confidence level, that corresponds to probability distribution (p) less than 0.05.

B. Description of the Dataset

To perform our study it is required to analyse as many different grasp postures as possible. In this way, a more general rule that applies to a large variety of grasping postures rather than to a limited set can be formulated. For this reason, data available in the GRASP database [22] was used for our analysis. The purpose of this dataset was to create a comprehensive taxonomy of grasp postures. Our study, instead, defines the role of the thumb in shaping human hand grasps and compares the freedom of movement of the thumb with the reachability space of the robotic thumbs.

The GRASP database captures 31 different grasp postures, and, therefore, the fingers span the majority of the possible positions used in grasping. As described in [18], five different subjects, all right handed, were asked to perform the grasp postures according to the classification outlined in [23]. The subjects, three males and two females, have an average hand length of 185.2 mm and hand width of 81.1 mm with standard deviation of 13.3 mm and 7.4 mm respectively. The objects used to perform each posture are listed on Table A in the Appendix. The subjects positioned their hand flat open with the dorsum up in front of the table. They were requested to replicate a grasp configuration as shown in a picture or, in case of difficulties, from the demonstration. During the grasping experiment, the hand approached the object, lifted it and was retreated back to the initial position after the object was placed down.

Each demonstration was recorded using Polhemus Liberty system with six magnetic sensors. The spatial and angular resolution of each sensor was 0.8 mm and 0.15 degrees respectively. A sensor was applied on each finger nail and one was placed on the dorsum of the hand, acting as reference point for the captured data as shown in Figure 1. The movements of the hand were recorded at 240 Hz. Each subject grasped

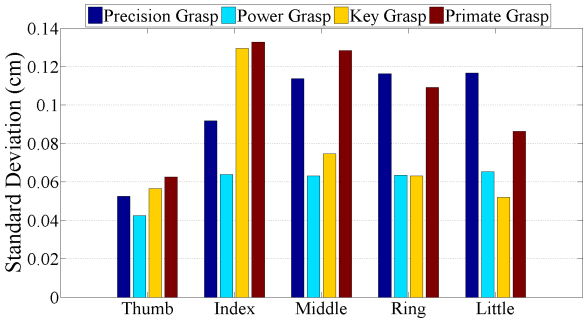

Fig. 3: Standard deviation of finger movements across the entire GRASP dataset [18]. The contribution given by each grasp posture class to its overall standard deviation is highlighted in different colour for each finger.

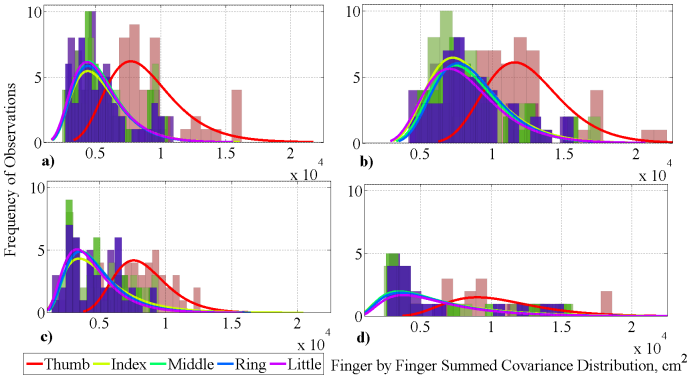

Fig. 4: Summed covariance between one fingertip and the fingertips of the other digits is displayed on the histograms along with the fitted distribution curve across all subjects and grasped objects. Figure *a)*, *b)*, *c)* and *d)* represents the results for power, precision, key and primate grasp classes respectively. Each colour represent a different digit. The closer the bars and the curves are to zero the less covariated is a specific finger while performing a specific grasp type. The higher a bar is, the more frequent is that specific motion coupling between a finger and the other digits. Each curve is a lognormal distribution fitted on the data of the GRASP dataset [18].

14 objects twice, each trial had 600 uniformly sampled data points.

C. Thumb-oriented Classification

The GRASP database uses a list of 31 different classes, that are partially derived from Cutlosky's posture classification [24]. In this paper, it was decided to simplify the list of possible postures to four, based on the employment of the thumb. This approach is required to highlight the role of the thumb in grasping for our analysis, and it was adopted from the classifications outlined by Pouydebat et al. [4] and by Napier [25]. Originally, Napier divided humanoid grasping in two categories - power and precision grasps. Pouydebat extended this classification to five categories based on the contact surface. Our classification takes into consideration the placement of the thumb with respect to the other four fingers. It also takes into account whether the grasp was performed using the fingertips only or the whole surface of the digits. The proposed classification uses thirty grasp postures, and each posture fits to one specific class out of four based on the functionality of the thumb. A comprehensive list of examples of our classification schema, and a comparison with the GRASP classification, can be found in Table A in the Appendix. The formulated posture classes are shown in Figure 2 and are defined as follows:

1) **Power Grasp:** the thumb opposes the other four fingers; the object is touched with the whole surface of the digits.
2) **Precision Grasp:** the thumb opposes at least one of the other four fingers; the object is touched with the fingertips only.
3) **Key Grasp:** the thumb does not oppose any of other fingers but is still used for prehension. There are no additional assumptions in respect to the other fingers.
4) **Primate Grasp:** the thumb is not used for grasping - its fingertip and most of the surface is not in contact with the object; the object is grasped using any of the other four fingers in any configuration. This posture class, along with the power grasp, is very popular among non-human primates but less frequently used by humans.

III. Analysis of Thumb Motion

A. Analysis of Variability of Movements of Fingers

As a first step, to explore the role of the thumb in prehensile grasping, the variability of each finger across postures and grasped objects was analysed. The standard deviation was calculated as follows. Initially, the 3D position of a finger was evaluated:

$$P_{f_{3\times1}} = R_{f_{3\times3}} T_{f_{3\times1}} \tag{1}$$

Where P_f is the 3D position of one data point of finger f and T_f and R_f are the translation and rotation components of finger f expressed in the dorsum reference frame. The calculation was performed on all the data points for all the trials of the dataset. Afterwards the norm of each 3D position was calculated:

$$N_f = |P_{f_{3\times1}}| \tag{2}$$

Where N_f is the Euclidean norm corresponding to 3D position P_f. The calculation was performed on each 3D position of the fingers for all the trials of the dataset. Finally, the trials were divided by grasping class, as indicated in Table A, and the standard deviation was calculated on the trials of a grasping class for each finger individually. Figure 3 shows the standard deviation of the norms of the three-dimensional displacement of the fingers across the whole dataset. The use of the norm allows to take into account both the magnitude and orientation of the fingertip positions with respect to the origin. Every coloured bar represents the variability of movements for each finger in a given grasp class. It is considered that the thumb is the most mobile digit of the hand [6]. However, Figure 3 demonstrates that the variability of motion of the thumb is the least across the four postures. The other fingers have more variability of motion in overall: the index finger -

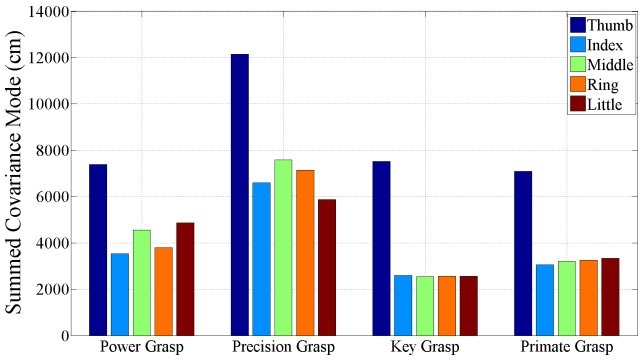

Fig. 5: Most frequent covariance (mode) per finger and posture class. The mode is calculated on the summation of the covariance for each posture class.

95% more than the thumb, the middle - 78%, the ring - 64%, and the little - 50%.

To evaluate the displacement of the thumb in relation to the other digits further, as well as to observe the influence of a posture class, the covariance of fingertip to fingertip positions was calculated for each trial of the dataset. The covariance for a single trial was calculated as follows:

$$C_{f_i,f_j} = E[(N_{f_i} - \mu_{N_{f_i}}) * (N_{f_j} - \mu_{N_{f_j}})] \tag{3}$$

Where N_{f_i} and N_{f_j} are the norms of the fingertip displacements of digit f_i and finger f_j respectively for a single trial, $\mu_{N_{f_i}}$ and $\mu_{N_{f_j}}$ are the means of finger f_i and finger f_j respectively for the trial, C_{f_i,f_j} is the covariance between digit f_i and digit f_j. The covariances were calculated among all the five fingers. For each finger, the covariances of the trials were grouped by grasping class as indicated in Table A and summed up to improve the representation:

$$S_g = \sum_{k=1}^{n} C^k_{f_i,f_j} \tag{4}$$

Where S_g is the summed covariance for grasping class g, $C^k_{f_i,f_j}$ is the covariance between finger f_i and finger f_j for trial k, n is the number of trials belonging to grasping class g. The results are shown as a histogram in Figure 4. Each sub-figure shows the results for the corresponding posture class, and each coloured bar represents a different finger. A lognormal distribution was fitted to the data to simplify the visual comparison of the covariances across fingers and posture classes. A lognormal distribution was chosen since it produced the best fit and the data is normally distributed. As a result, Figure 4 highlights the strong magnitude of covariance between the thumb and the other digits. In other words, the motion of the thumb is leading the displacement of the other fingers. In addition, this trend can be observed in all four posture classes. The thumb is the digit that shows less variability of motion across the four posture classes. Therefore, the contribution to the high covariance values of the thumb motion must come primarily from the other four fingers. This suggests that the motion of the other four digits follows the motion of the thumb.

TABLE I: Summary of ANOVA test results on the GRASP database [18]. F is the value of the Fisher's index, while p is the P-value. Entries in bold are statistically significant.

Finger	Posture		Subject		Object	
	F	p	F	p	F	p
Thumb	**5.94**	**<0.02**	0.28	0.6	0.61	0.44
Index	**3.58**	**<0.01**	**3.05**	**<0.01**	**7.91**	**<0.0001**
Middle	1.62	0.2	0.29	0.59	**5.46**	**<0.001**
Ring	**3.48**	**<0.01**	3.05	0.92	0.75	0.39
Little	**4.35**	**<0.01**	0.65	0.42	0.07	0.79

To further validate the leading role of the thumb for each grasping posture, the most frequent covariance values (modes) per finger and grasping posture, obtained from the histogram (Figure 4), are compared. The mode is the value occurring most frequently in the distribution. The mode of covariance distribution for each finger was calculated and shown in Figure 5. The diagram confirms that the motion of the thumb is more interdependent with the motion of the other fingers.

In summary, our analysis in this section shows that the movement of the thumb during grasping is less compared to the displacement of the other fingers (Figure 3), but at the same time the displacement of the other fingers strongly depends on the displacement of the thumb (Figure 4). In addition, the motion of the thumb is the most interdependent with the other fingers (Figure 5). These findings demonstrate that the displacement of the thumb is a determining factor for the motion of the other fingers in grasping.

B. Statistical Evaluation

To verify our results on the prominent role of the thumb statistically, ANOVA tests were performed. The statistical analysis was performed to verify whether additional conditions can influence the variance of motion of each finger. In this case, the additional conditions are - the object being grasped, the subject performing the grasp, and one of the four assigned postures. The purpose of this analysis is to add further evidence to our findings in previous section that state that the thumb motion has a prominent role in shaping the hand grip. Results of the ANOVA test are shown in Table I.

The strongest dependency on the variability of the thumb position is the posture executed by a subject to grasp an object ($F_{(1,150)} = 5.94,\ p < 0.02$). The object ($F_{1,150} = 0.61,\ p = 0.44$) and the subject ($F_{1,150} = 0.28,\ p = 0.6$) are statistically not influencing the thumb position. The displacement of other fingers, such as the index ($F_{1,150} = 3.58,\ p < 0.01$), the ring ($F_{1,150} = 3.48,\ p < 0.01$) and the little ($F_{1,150} = 4.35,\ p < 0.01$), are also playing a significant role. In addition, we can observe that there is a strong dependency from the object for index ($F_{1,150} = 7.91,\ p < 0.0001$) and middle ($F_{1,150} = 5.46,\ p < 0.001$) fingers. Such dependency from the object might be used to interpret the specific geometry of the grasped object.

Similarly to the thumb, the ring and little fingers are only posture dependent. However, these two fingers are only employed in 63.3% and 53.3% out of all the grasping demonstrations respectively. Conversely, the thumb is used in 90% of the grasping executions. Therefore, the results of the statistical

evaluation highlight the broad use of the thumb, that is independent from the grasped object. In other words similar motion of the thumb can be used to grasp different shapes.

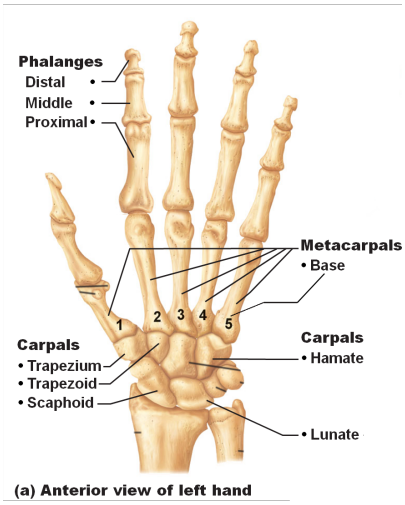

(a) Schema depicting the 26 bones of the human hand. Bones referenced in text are reported on the figure.

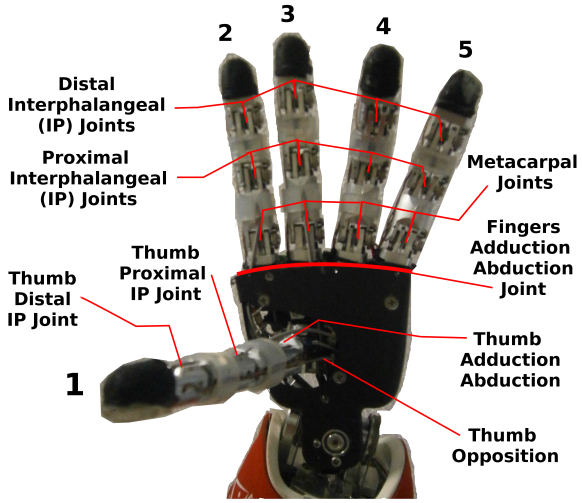

(b) Diagram of the iCub hand kinematics.

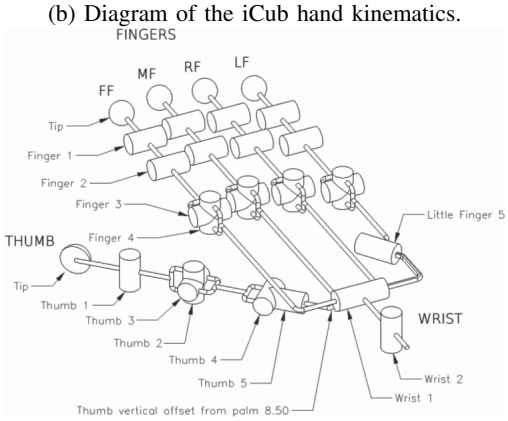

(c) Diagram of the Shadow hand kinematics.

Fig. 6: Diagrams of human hand skeleton and the iCub and Shadow hand kinematics ((C) Shadow Robot Company 2014). The kinematics of the iCub hand thumb has four DoFs and is under-actuated, while the kinematics of the Shadow hand thumb has five DoFs and is fully actuated.

To summarize, the index and the middle fingers can provide information on the object geometry, while the thumb motion can determine which grasp posture is used. The posture can be used to grasp a possible set of objects. For instance, the same thumb motion is suitable to grasp to transport a cylindrical pole and a flat rectangular crowbar. The index and middle fingers can distinguish whether the subject is grasping the crowbar or the pole.

IV. Human-Robot Thumb Reachability Space Comparison

A. Motivation

In this section, we investigate whether state-of-the-art robotic thumbs are representing the motion of the human thumb evenly across posture classes. It is required to evaluate the reachability space of robotic thumbs compared to the human thumb. The iCub [26] and the Shadow [13] robotic hand were used for the analysis. The main reason behind this choice is that those two hands model the kinematic of the thumb similarly to other multifingered human-like robotic hands. For instance, the Robonaut 2 Hand [27], Gifu Hand [28], HIT/DLR Hand 2 [14] and Sandia Hand [29] are some of the examples. The kinematic chain of the thumb of the above mentioned hands is inspired by the morphology of the human thumb. The human thumb can oppose to the other fingers, as the region of the trapezium, trapezoid and scaphoid can be folded [6]. It can also be adducted and abducted around the distal and proximal articulations. These motions are of interest for our analysis. Additionally, the two selected hands are a commercial application and a scientific prototype, and their kinematic design is freely available for analysis.

Our study considers robotic hands with a thumb opposition joint placed at the base of the thumb proximal phalanx, near the articulation of the thumb metacarpal (see Figure 6a). The same kinematic design of the opposition joint of the thumb is used in the above mentioned hands. The iCub hand has a four Degrees of Freedom (DoFs) thumb, as shown in Figure 6b, and the Shadow hand has a five DoFs thumb, as shown in Figure 6c. The analysis of the reachability space of these two robotic thumbs can give a better understanding of the rendering of the thumb motion in robotics.

It is worth to mention that other human-inspired multifingered grippers, such as the Barrett Hand [15] or the metamorphic hand [30] are not considered in this study. This is because of the use of a grasping principle different from human morphology. For example, the fingers of the Barrett Hand synchronously rotate around the palm surface, and the metamorphic hand has a reconfigurable metamorphic palm that allows complex configuration of the fingers different from human morphology.

B. Methodology of Analysis

In this part, the methodology used to compare the reachability spaces of human and robot thumbs is described. The first step for the comparison of reachability spaces of the human and robot thumbs is to calculate all the positions of the tip of the robotic thumb in 3D space. The forward kinematics of

the robotic thumbs were calculated numerically using standard equations [31] with the Denavit-Hartenberg (DH) parameters of the two hands. The origin frame of the kinematic chains of the thumbs was set to the centre of the dorsum of each respective robotic hand, so that the calculated thumb positions for both hands are expressed in the dorsum reference frame. The DH parameters of the Shadow Hand were obtained from the work of L. Cui et al. [32] and the joint values were taken from the Shadow Hand Technical Specifications [13]. The origin frame was translated from the origin reference point of 280 mm on the Z axis. The DH parameters and the joint values of the iCub hand were obtained from the iCub online manual [33]. The origin frame was translated from the reference point of -4.3 mm, -3.3 mm and -19.1 mm on the X, Y and Z axes respectively. The reachability space of the iCub hand was calculated using all available joint values using one degree step. The reachability space of the Shadow hand was evaluated using intervals of 5 degrees due to the high computational complexity of the calculation. The total number of data points generated from the calculations are of comparable size: 670,761 and 504,735 for the iCub and the Shadow hand respectively. The size of the iCub hand is slightly smaller than an average human hand. Therefore, it was required to isotropically scale up the data calculated from the iCub forward kinematics by a 1.23 factor. This coefficient was calculated by dividing the length of the iCub hand (165 mm) by the mean length of male hand (197.1 mm according to [34]) and inverting the resulting scaling matrix.

The human hand is a biological gripper and its reachability space can be described as a function of many subject dependent variables, such as elasticity of tendons, cartilaginous flexibility of the articulations, length of the bones, tendons and muscles and more. Therefore, the reachability space of the human thumb cannot be calculated in closed form in general. It is possible to calculate the reachability space of the human thumb using a specific kinematic model from literature. However, in our analysis, the reachability space was derived from the thumb motion data of the GRASP database to avoid any bias and inaccuracies imposed by a kinematic model. Human data from the primate grasp posture class was excluded from this analysis, as the thumb is not used in prehensile movements by definition of this posture.

The human and robot data were divided in three groups, one for each plane of the 3D space, in order to simplify the comparison of the reachability spaces. The human and robot reachability spaces were expressed as point clouds. For each 3D plane, the point clouds were enveloped by the minimum convex hull that represents the minimum fit to the point cloud; while a regular convex hull can be of any dimension. The approximation to convex hulls is used, as the point cloud for human and robot reachability spaces is nearly convex. As a result, we have obtained three convex hulls for each human posture class (power, precision and key grasp), and two convex hulls for each robot hand. The two robot hands were compared with the human data separately, as can be seen in Figure 7. The comparison was based on their geometrical overlap with the reachability spaces of the human thumb and it was calculated numerically. Additionally, the volumes of 3D reachability spaces of the human thumb for the Power and Precision Grasp reachability spaces and the volumes of the robotic thumb reachability spaces were compared to the mean palm area. The mean palm area was calculated as *palm length* $\times$ *palm width* using data collected in [34] from more than 1000 male subjects. The mean palm length is $110.5mm$ and the mean palm width is $95.3mm$. The volumes of the 3D reachability spaces were calculated on the minimum convex hull enveloping the point clouds in 3D spaces. The Key Grasp was excluded as the thumb is not opposing the other fingers by definition and it would be inappropriate to compare it to the area of the palm. This comparison is defined as spanning ratio and was calculated as follows:

$$\frac{V_h}{A_p} \tag{5}$$

Where A_p is the mean palm area and V_h is the volume of the convex hull of any reachability space used in the comparison (Table III).

The area of the intersection was calculated using the Sutherland-Hodgman algorithm [35] if the convex hull of a robot hand overlapped the convex hull of human posture class. This algorithm, widely used in computer graphics, calculates the intersection between two polygons - a clipping polygon and a subject polygon. In our case, the clipping polygon was the robot hand convex hull and the subject polygon was a human posture class convex hull. The intersection area was calculated for each posture class and for each plane across the two robot hands. An intersection area was expressed as a percentage of coverage by dividing it by the corresponding human posture class area. Then, the total percentage of coverage for each posture class was calculated as the average across the three planes.

C. Comparison of Human-Robot Reachability Spaces

This part shows the results of our numerical comparison to evaluate whether the selected robotic thumbs are evenly spanning across the reachability space of human thumb for each posture class. Figure 7 shows the reachability spaces expressed as convex hulls for each human posture class and robot thumb across the three planes. From this figure, it can be observed that the reachability spaces of the robot thumbs are not covering evenly the reachability spaces of human thumb. As the Shadow Hand is more articulated than the iCub hand, a larger space of the human data is covered, but still the space does not evenly correspond to the human reachability space for all posture classes. Both hands do not perform well when covering the motion in the side view (XZ plane), as shown in Figure 7c and Figure 7f.

In addition, it can be observed that the key grasp is the most under-represented category of grasps in robotic thumbs. It is covered only by 35.7% and 2% of the Shadow and iCub hand reachability space. The best represented class is the precision grasp, covered by 46.65% and 3.15% of the reachability spaces of the Shadows and iCub hand respectively. The results of the representation by robotic thumbs for each grasping class are reported in Table II. These findings can be explained by the

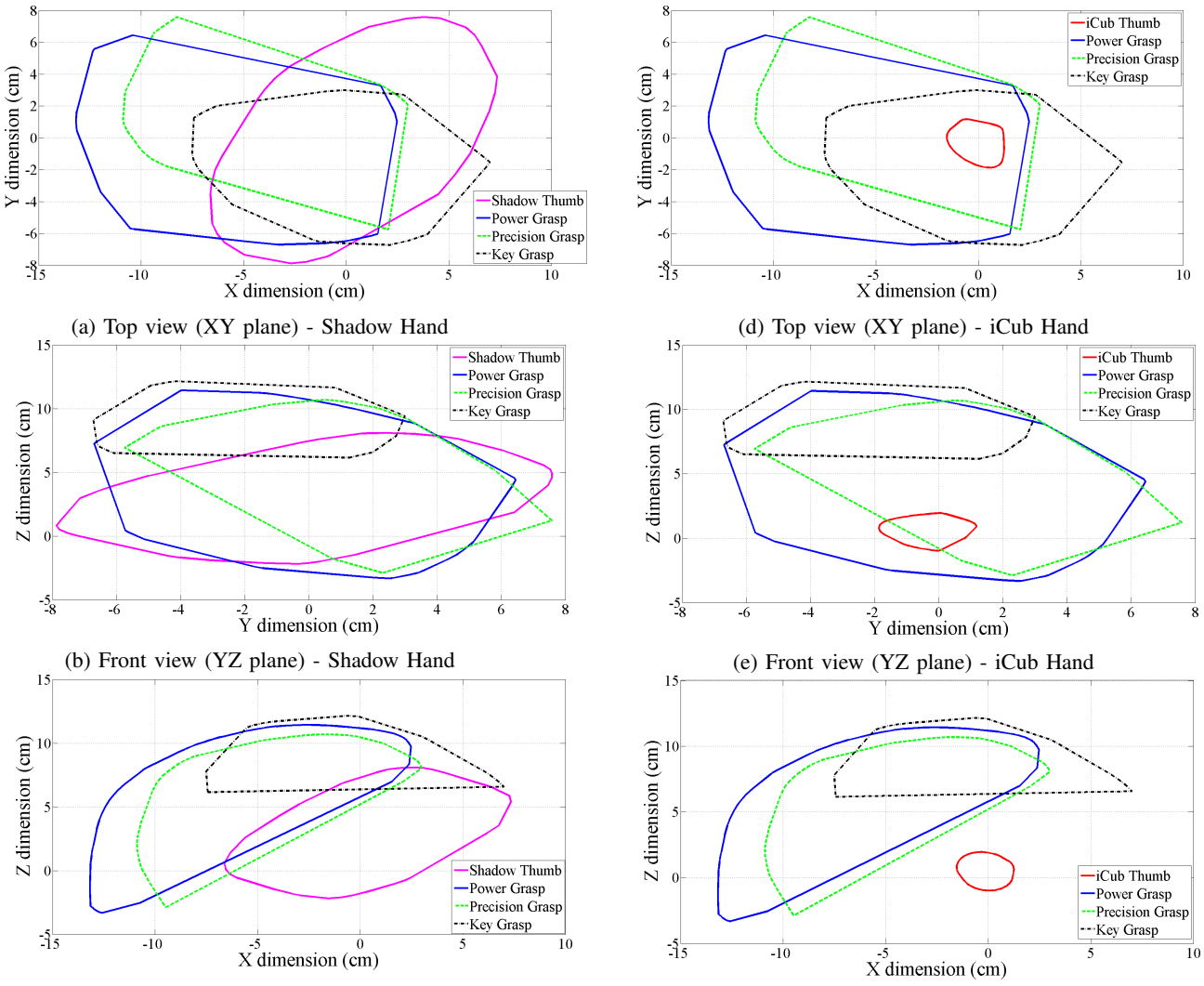

(a) Top view (XY plane) - Shadow Hand

(d) Top view (XY plane) - iCub Hand

(b) Front view (YZ plane) - Shadow Hand

(e) Front view (YZ plane) - iCub Hand

(c) Side view (XZ plane) - Shadow Hand

(f) Side view (XZ plane) - iCub Hand

Fig. 7: The figures compare the human thumb reachability space, derived from the GRASP database captures and organised by posture class, with the Shadow thumb reachability space (continuous magenta line) and iCub thumb reachability space (continuous red line) calculated from their respective forward kinematics. The polygons represent the minimum convex hull enveloping the data samples. The primate grasp posture class has been excluded from the calculation as the thumb is not relevant for grasping by definition.

TABLE II: Summary of the percentage of overlaps between robot thumb reachability space and human thumb reachability space divided by posture class.

Grasping Class	Shadow Hand	iCub Hand
Power Grasp	41.02%	2.63%
Precision Grasp	46.65%	3.15%
Key Grasp	35.73%	2%

fact that robotic grasping is traditionally focussed on contact-point based precision grasping. Hence, the design principles of robotic hands are more adequately representing this category of grasps.

V. Discussion

In this paper we quantified the role of the thumb in prehensile grasping. Our analysis of motion variability demonstrated that the motion of the thumb is leading the motion of the other fingers in grasping, and that the thumb position depends only on the specific configuration of the grasp, independently of the object. This answers our first question proposed in this paper: the motion of the thumb influences the shape of the grip independently from the object being grasped.

Additionally, to explore our second question about the coverage of the reachability space between human and robot thumbs, we compared the prehensile reachability space of the human thumb with the reachability space of two robotic hands, the iCub hand and the Shadow hand. The Shadow hand is considered one of the most dexterous robotic hands available, but our analysis shows that the representation of the reachability space of the human thumb is below the half in case of all posture classes. Additionally, the volumes of the reachability spaces of the robotic thumbs and of the human thumb were compared alongside with the spanning ratio between the volumes and mean area of the male palm. It can be observed from the results in Table III that the surface of the palm covered by human power grasp is larger than

TABLE III: Summary of the volumes of the 3D convex hull enveloping the reachability spaces and the spanning ratio between area of the palm and volumes of the hulls.

3D Convex Hull	Volume (mm^3)	Spanning Ratio
Power Grasp	956.1	0.0916
Precision Grasp	627.4	0.0596
Human Overall	1157.1	0.1099
Shadow Hand	757.6	0.0719
iCub Hand	11.3	0.0011

the surface covered by the Shadow Hand thumb as the ratio between the volume of the reachability space of the Power Grasp and the area of the palm is larger than the ratio between the reachability space of the Shadow Hand thumb and the area of the palm. However, the situation is inverted for the Precision Grasp reachability space. In this case the Shadow Hand thumb spans a larger area than the human reachability space. Overall the spanning ratio of the Shadow Hand is much inferior to the human thumb. We found that precision grasp is the best rendered posture and key grasp is the least represented posture, as also shown by the overlap between the human and robot reachability spaces.

A possible explanation to the better representation of Precision Grasp posture can be found in the way robotic grasping was performed historically. Originally, robotic grasping algorithms were focussing on the optimal placement of the fingertips on the geometrical surface of an object [36]. As robotic hand design is increasingly more focussed on mechanical implementations of human grasping synergies [16] it could be appropriate to modify the design of robotic thumbs to better represent other posture classes such as Power Grasp.

Humans are the only primates that are able to manipulate objects in a very complex way, and most of everyday objects are tailored to our needs. Therefore, it is likely that robotic thumbs will be better poised to manipulate objects that are designed for human hands if they capture the essential morphological features of human thumb. In this case, we would like to highlight that the kinematics of future robotic grippers should consider extending the thumb reachability space by opposing the whole trapezium-trapezoid-scaphoid complex, as it is in humans, rather than just opposing the base of the thumb metacarpal.

However, it is worth to note that it is possible to perform suitable grasps without the need of using the thumb, as is the case for many primates. Such approach is limited to the use of one posture class only (primate grasp), hence reducing the dexterity of manipulation.

It is worth to mention that there is an extensive research on the sharing of forces between in grasping using different postures. The central nervous system balances synergistically the force contribution of each finger if the grip is perturbed [37]. If a power grasp is used the forces are shared among the phalanxes of the fingers [38]. The force sharing and the point of application of the grip force changes if the thumb is not used for grasping [39]. If the hand is grasping a hold during rock climbing, the thumb is not considered as an independent force actuator, but its force contribution is combined with the index finger as they would be a unique actuator (i.e. virtual finger) [40]. It could be that the force sharing mechanism across different fingers could have an impact in determining the leading role of the thumb. This point however was not explored in this study, as it is out of scope. A separate study is required to better understand the impact of different finger forces in grasping.

VI. Conclusions

To summarise, this paper can be used as an indication of future directions for the design of robotic hand kinematics, as it highlights the important role of the human thumb. In addition a classification based on thumb position in respect to the grasped object was outlined.

As future work the time of contact between the fingers and the object and the speed of the motion will be studied to better understand the temporal relationship between fingers in grasping. Also the force sharing between fingers will be taken into consideration.

Acknowledgment

The research leading to these results has received funding from the European Community's Seventh Framework Programme (FP7/2007-2013) project DARWIN (Grant No: FP7-270138). Authors would like to thank the EU FP7 GRASP consortium, the Robotcub Hackers community and Shadow Company for the useful discussions.

References

[1] T. Okada, "Computer Control of Multijointed Finger System for Precise Object-Handling," *IEEE Transactions on Systems Man and Cybernetics*, vol. 75, no. 3, pp. 289–299, 1982.

[2] M. W. Marzke, "Precision grips, hand morphology, and tools," *American Journal of Physical Anthropology*, vol. 102, no. 1, pp. 91–110, 1997.

[3] M. W. Marzke and R. F. Marzke, "Evolution of the human hand: approaches to acquiring, analysing and interpreting the anatomical evidence." *Journal of anatomy*, vol. 197 (Pt 1), pp. 121–40, Jul. 2000.

[4] E. Pouydebat, M. Laurin, P. Gorce, and V. Bels, "Evolution of grasping among anthropoids." *Journal of evolutionary biology*, vol. 21, no. 6, pp. 1732–43, Nov. 2008.

[5] R. W. Young, "Evolution of the human hand: the role of throwing and clubbing," *Journal of Anatomy*, vol. 202, no. 1, pp. 165–174, 2003.

[6] I. Kapandji, *The Physiology of the Joints: Upper limb*, ser. Physiology of the Joints. Churchill Livingstone, 1982.

[7] K. Kuczynski, "Carpometacarpal joint of the human thumb." *Journal of anatomy*, vol. 118, no. Pt 1, p. 119, 1974.

[8] W. P. Cooney, M. J. Lucca, E. Chao, and R. Linscheid, "The kinesiology of the thumb trapeziometacarpal joint." *The Journal of Bone & Joint Surgery*, vol. 63, no. 9, pp. 1371–1381, 1981.

[9] D. TC and H. TP, *Guides to the evaluation of permanent impairment 3rd ed.* American Medical Association Press, 1993.

[10] E. T. Emerson, T. J. Krizek, and D. P. Greenwald, "Anatomy, physiology, and functional restoration of the thumb," *Annals of plastic surgery*, vol. 36, no. 2, pp. 180–191, 1996.

[11] M. Bianchi, P. Salaris, and a. Bicchi, "Synergy-based hand pose sensing: Optimal glove design," *The International Journal of Robotics Research*, vol. 32, no. 4, pp. 407–424, Apr. 2013.

[12] E. P. Pitarch, "Virtual Human Hand : Grasping Strategy and Simulation," Ph.D. dissertation, Universitat Politecnica de Catalunya, 2007.

[13] "Shadow Dexterous Hand E1 Series, Technical Specification," Shadow Company, Tech. Rep. January, 2013.

[14] H. Liu, P. Meusel, N. Seitz, B. Willberg, G. Hirzinger, M. Jin, Y. Liu, R. Wei, and Z. Xie, "The modular multisensory dlr-hit-hand," *Mechanism and Machine Theory*, vol. 42, no. 5, pp. 612 – 625, 2007.

[15] W. Townsend, "The BarrettHand grasper - programmably flexible part handling and assembly," *Industrial Robot: An International Journal*, vol. 27, no. 3, pp. 181–188, 2000.

[16] G. Grioli, M. Catalano, E. Silvestro, S. Tono, and A. Bicchi, "Adaptive synergies: An approach to the design of under-actuated robotic hands," *2012 IEEE/RSJ International Conference on Intelligent Robots and Systems*, pp. 1251–1256, Oct. 2012.

[17] C. Y. Brown and H. H. Asada, "Inter-finger coordination and postural synergies in robot hands via mechanical implementation of principal components analysis," *2007 IEEE/RSJ International Conference on Intelligent Robots and Systems*, pp. 2877–2882, Oct. 2007.

[18] T. Feix, J. Romero, C. H. Ek, H.-B. Schmiedmayer, and D. Kragic, "A Metric for Comparing the Anthropomorphic Motion Capability of Artificial Hands," *IEEE Transactions on Robotics*, vol. 29, no. 1, pp. 82–93, Feb. 2013.

[19] G. Salvietti, M. Malvezzi, G. Gioioso, and D. Prattichizzo, "On the use of homogeneous transformations to map human hand movements onto robotic hands," in *Proc. IEEE Int. Conf. on Robotics and Automation, no. 0,(Hong Kong, China)*, 2014.

[20] G. Cotugno, V. Mohan, K. Althoefer, and T. Nanayakkara, "Simplifying Grasping Complexity Through Generalization of Kinaesthetically Learned Synergies," in *Proceedings of 2014 IEEE International Conference on Robotics and Automation*, 2014.

[21] G. Cotugno, J. Konstantinova, K. Althoefer, and T. Nanayakkara, "On the Dexterity of Robotic Manipulation : Are Robotic Hands Ill Designed ?" in *Proceeding of the 6th International Conference on Cognitive Science*, Kaliningrad, 2014.

[22] T. Feix, R. Pawlik, H. Schmiedmayer, J. Romero, and D. Kragic, "A comprehensive grasp taxonomy," in *Robotics, Science and Systems: Workshop on Understanding the Human Hand for Advancing Robotic Manipulation*, June 2009. [Online]. Available: http://grasp.xief.net

[23] EU FP7 GRASP Project Consortium, "Human Grasping Database," http://grasp.xief.net/, September 2014.

[24] M. Cutkosky, "On grasp choice, grasp models, and the design of hands for manufacturing tasks," *IEEE Transactions on Robotics and Automation*, vol. 5, no. 3, pp. 269–279, Jun. 1989.

[25] J. R. Napier, "The prehensile movements of the human hand," *Journal of bone and joint surgery*, vol. 38, no. 4, pp. 902–913, 1956.

[26] A. Schmitz, U. Pattacini, F. Nori, L. Natale, G. Metta, and G. Sandini, "Design, realization and sensorization of the dexterous iCub hand," in *10th IEEE-RAS International Conference on Humanoid Robots*. Ieee, Dec. 2010, pp. 186–191.

[27] M. Diftler, J. Mehling, M. Abdallah, N. Radford, L. Bridgwater, A. Sanders, R. Askew, D. Linn, J. Yamokoski, F. Permenter, B. Hargrave, R. Piatt, R. Savely, and R. Ambrose, "Robonaut 2 - the first humanoid robot in space," in *Robotics and Automation (ICRA), 2011 IEEE International Conference on*, May 2011, pp. 2178–2183.

[28] H. Kawasaki, T. Komatsu, and K. Uchiyama, "Dexterous anthropomorphic robot hand with distributed tactile sensor: Gifu hand II," *IEEE/ASME Transactions on Mechatronics*, vol. 7, no. 3, pp. 296–303, Sep. 2002.

[29] M. Quigley, C. Salisbury, A. Y. Ng, and J. K. Salisbury, "Mechatronic design of an integrated robotic hand," *The International Journal of Robotics Research*, vol. 33, no. 5, pp. 706–720, 2014.

[30] G. Wei, J. S. Dai, S. Wang, and H. Luo, "Kinematic analysis and prototype of a metamorphic anthropomorphic hand with a reconfigurable palm," *International Journal of Humanoid Robotics*, vol. 8, no. 03, pp. 459–479, 2011.

[31] J. Denavit and R. S. Hartenberg, "A kinematic notation for lower-pair mechanisms based on matrices," *Journal of Applied Mechanics*, 1955.

[32] L. Cui, U. Cupcic, and J. S. Dai, "An optimization approach to teleoperation of the thumb of a humanoid robot hand: Kinematic mapping and calibration," *Journal of Mechanical Design*, vol. 136, no. 9, p. 091005, 2014.

[33] RobotCub Wiki, "iCub Right Hand Forward Kinematics," http://wiki.icub.org/wiki/ICubFowardKinematics_hand_right, September 2014.

[34] T. M. Greiner, "Hand anthropometry of U.S. army personnel," United States Army Natick Research, Development and Engineering Center, Tech. Rep., 1991.

[35] I. E. Sutherland and G. W. Hodgman, "Reentrant polygon clipping," *Communications of the ACM*, vol. 17, no. 1, pp. 32–42, 1974.

[36] K. B. Shimoga, "Robot grasp synthesis algorithms: A survey," *The International Journal of Robotics Research*, vol. 15, no. 3, pp. 230–266, 1996.

[37] G. P. Slota, M. L. Latash, and V. M. Zatsiorsky, "Tangential finger forces use mechanical advantage during static grasping," *Journal of applied biomechanics*, vol. 28, no. 1, 2012.

[38] B. G. de Monsabert, J. Rossi, E. Berton, and L. Vigouroux, "Quantification of hand and forearm muscle forces during a maximal power grip task," *Medicine and science in sports and exercise*, vol. 44, no. 10, pp. 1906–1916, 2012.

[39] L. Vigouroux, J. Rossi, M. Foissac, L. Grélot, and E. Berton, "Finger force sharing during an adapted power grip task," *Neuroscience letters*, vol. 504, no. 3, pp. 290–294, 2011.

[40] F. Quaine, L. Vigouroux, F. Paclet, and F. Colloud, "The thumb during the crimp grip," *International journal of sports medicine*, vol. 32, no. 1, p. 49, 2011.

APPENDIX

The table shows the mapping between our posture class defined in section II-C and the GRASP nomenclature as in the database [18]. For each entry of the GRASP database it is showed the GRASP nomenclature, our corresponding classification, a pictorial representation of the posture (from the description of the GRASP online database [22]), the object grasped to produce the posture and the GRASP identification number used in the database.

Posture class	GRASP name	Picture	Grasped Object	Posture class	GRASP name	Picture	Grasped Object
Power Grasp	Large diameter		Cylinder (11cm diameter)	Key Grasp	Adducted Thumb		Cylinder (3cm diameter)
Power Grasp	Small diameter		Cylinder (3cm diameter)	Key Grasp	Light Tool		Cylinder (1cm diameter)
Power Grasp	Medium Wrap		Cylinder (3cm diameter)	Key Grasp	Lateral		Credit Card
Power Grasp	Power Disk		MiniDisc (8cm diameter, 2mm tall)	Key Grasp	Index Finger Extension		Cylinder (3cm diameter)
Power Grasp	Power Sphere		Tennis Ball (6.7cm diameter)	Key Grasp	Writing Tripod		Cylinder (1cm diameter)
Power Grasp	Parallel Extension		Box (4cm thick)	Key Grasp	Sphere 3 Fingers		Tennis Ball (6.7cm diameter)
Power Grasp	Lateral Tripod		Bottle Cap	Key Grasp	Stick		Cylinder (1cm diameter)
Power Grasp	Sphere 4 Fingers		Tennis Ball (6.7cm diameter)	Key Grasp	Ventral		Cylinder (1cm diameter)
Power Grasp	Ring		Cylinder (6.4cm diameter)	Primate Grasp	Fixed Hook		Cylinder (3cm diameter)
Power Grasp	Inferior Pincer		Golf Ball (4.3cm diameter)	Primate Grasp	Adduction Grip		Cylinder (1cm diameter)
Precision Grasp	Prismatic 4 Fingers		Cylinder (1cm diameter)	Primate Grasp	Palmar		Plate
Precision Grasp	Prismatic 3 Fingers		Cylinder (1cm diameter)	Not used	Extension Type		Plate
Precision Grasp	Prismatic 2 Fingers		Cylinder (1cm diameter)				
Precision Grasp	Palmar Pinch		Coin				
Precision Grasp	Precision Disk		Compact Disc				
Precision Grasp	Precision Sphere		Tennis Ball (6.7cm diameter)				
Precision Grasp	Tripod		Golf Ball (4.3cm diameter)				
Precision Grasp	Tip Pinch		Cube 5mm				
Precision Grasp	Quadpod		Golf Ball (4.3cm diameter)				

Giuseppe Cotugno obtained his bachelor degree in Computer Engineering from the University of Calabria, Cosenza, Italy, in 2007 and his master degree in Computer Engineering from the University of Rome La Sapienza, Rome, Italy, in 2010. He was member of the Italian Robocup football team (SPQR team) in the Standard Platform League in 2009 at University of Rome La Sapienza, he was visiting researcher at Humboldt University Berlin in 2010 and he was Robotic Manipulation Team Leader of the KCL DARPA Team at King's College London in 2013. He is currently working towards his Ph.D. degree in Robotics at King's College London. His research interests are robotic manipulation and grasping, grasp and object affordances, learning by demonstration and reinforcement, humanoid robotics and applications of neuroscience to robotics and engineering.

Kaspar Althoefer holds a Degree in electronic engineering from the University of Aachen, Aachen, Germany, and the Ph.D. degree in electronic engineering from Kings College London, London, U.K. He is currently a Professor of Robotics and Intelligent systems at Kings College London and Head of the Center for Robotic Research (CoRe). His research interests are force and tactile sensors for medical applications, miniaturised optic-fibre-based sensing, medical robotics, flexible and continuum robots, and neuro-fuzzy sensor signal analysis and classification.

Thrishantha Nanayakkara received the BSc and MSc degrees in electrical engineering from the University of Moratuwa (UM), Sri Lanka (1996), and Saga University (SU), Japan (1998), and PhD in robotics from SU (2001). He was a postdoctoral research fellow in the department of biomedical engineering, Johns Hopkins University, USA, 2001-2003; a senior lecturer in the faculty of engineering at the UM; a Radcliffe Fellow at Harvard University, USA (2008/09), and a research affiliate at MIT (2008/09), USA. He is currently a senior lecturer in the department of Informatics, Kings College London. His research interests are in soft robotics, and robotic interaction with uncertain environments. He has published one textbook and more than 80 peer reviewed papers.